Dynamics of Pore Growth in Membranes and Membrane Stability

W. Sung and P. J. Park
Department of Physics, Pohang University of Science and Technology, Pohang 790-784, Korea

ABSTRACT Pores can form and grow in biomembranes because of factors such as thermal fluctuation, transmembrane electrical potential, and cellular environment. We propose a new statistical physics model of the pore growth treated as a non-Markovian stochastic process, with a free energy barrier and memory friction from the membrane matrix treated as a quasi-two-dimensional viscoelastic and dielectric fluid continuum. On the basis of the modern theory of activated barrier crossing, an analytical expression for membrane lifetime and the phase diagram for membrane stability are obtained. The memory effect due to membrane viscoelasticity and the elasticity due to cytoskeletal network are found to induce sharp transitions to membrane stability against pore growth and compete with other factors to manifest rich dynamic transitions over the membrane lifetime.

INTRODUCTION

The lipid bilayer membrane is a quasi-two-dimensional flexible structure that undergoes a variety of structural and dynamic transitions (Sackmann et al., 1993). A pore can form and grow in membrane in response to thermal fluctuation and external influences. Pore growth induced by strong electric fields applied to cells, called electroporation, dramatically enhances the transport of macromolecules such as proteins, DNAs, and other genetic materials, as well as ions, across the membranes. The electroporation as well as the fusion of these electrically destabilized membranes bring about novel biotechnological applications such as gene transfer and cell fusion (Neumann et al., 1989; Chang et al., 1992).

To our knowledge, only a few theoretical studies have been done to gain a physical understanding of pore growth (Sugar and Neumann, 1984; Dimitrov, 1984; Abidor et al., 1979) and related phenomena (Safran and Klein, 1993; Freeman et al., 1994; Tsong, 1991), despite much research effort directed toward this biologically and biotechnologically important problem (Neumann et al., 1989; Chang et al., 1992). As complex as the pore and its environment are (Fig. 1), a quantitative explanation of these phenomena in terms of measurable, minimal free parameters is challenging and yet, lacking, in our view. In this paper we intend to develop a new theory in the light of statistical physics of stochastic processes to elucidate the effects of thermal fluctuations, membrane and environment, and, most importantly, membrane viscoelasticity, cytoskeleton, as well as transmembrane potential. For analytical tractability, we consider the case of a single pore already formed in a membrane (either model or biological), both of which are immersed in solvent (water) under constant electric potential. Although this consideration is not directly applicable to experimental situations with the usual electroporation measurements in which the applied fields are time dependent, this nevertheless can contribute to understanding the pore growth mechanism in a broad range of situations, not to mention the natural situation of membrane under constant resting potential.

In our mesoscopic description over length scales much larger than the size of lipid molecules, we treat the membrane as a two-dimensional dielectric and viscoelastic fluid continuum responding dynamically to pore growth. The free energy required to form a pore of radius r in a membrane is given by (Litster, 1975)

$$\mathcal{A}(r) = 2\pi\lambda r - \pi\sigma r^2 \tag{1}$$

where λ is the energy cost of forming a pore edge per unit length (line tension) and σ is the membrane surface tension. As can be seen from microscopic models (Kashchiev, 1987), these parameters have definite molecular definitions. For example, the surface tension σ is given by the chemical potential difference of a lipid molecule between solution and membrane phases. The parameters λ and σ depend on the transmembrane potential U, as shown in Eqs. 23 and 24 (Winterhalter and Helfrich, 1987).

This free energy alone gives a rough estimate of the stability condition of the pore. For $r < r_B$, where $r_B \equiv \lambda/\sigma$ is the pore radius for the maximum free energy, the radial force associated with a change in radius,

$$F_A = -\frac{\partial}{\partial r}\mathcal{A}(r) = k(r - r_B) \tag{2}$$

with $k = 2\pi\sigma > 0$ tends to reseal the pore, and the membrane becomes stable against pore growth (Fig. 2). On the other hand, a pore with a radius $r > r_B$ undergoes indefinite growth, leading ultimately to a membrane breakdown. Incorporating thermal fluctuation into this naive picture, one can view the pore radius r as a Brownian process crossing the barrier of free energy $\mathcal{A}(r)$. In view of the barrier lowered by transmembrane potential in Fig. 2, one

Received for publication 30 May 1996 and in final form 25 June 1997.

Address reprint requests to Dr. W. Sung, Department of Physics, Pohang University of Science and Technology, Pohang 790-784, Korea. Tel.: 82-562-279-2061; Fax: 82-562-279-3099; E-mail: sung@galaxy.postech.ac.kr.

0006-3495/97/10/1797/08 $2.00

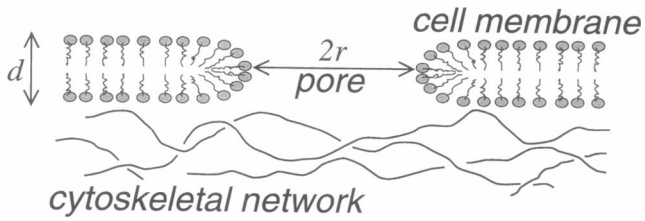

FIGURE 1 A schematic cross-sectional view of a pore in a cell membrane with cytoskeletal network.

can see how the pore can be destabilized by the potential. However, this explanation is not complete unless one does incorporate the effect of friction on pore operating on the time scale of growth. In a quantitative theory presented here, the memory friction arising from membrane viscoelasticity gives rise to a significant stability against pore growth, when k is sufficiently small.

In this paper we treat pore growth as a non-Markovian stochastic process crossing the free energy barrier given by Eq. 1. In the next section, we set up a generalized Langevin equation for pore radius, which involves the memory function as well as the free energy. The membrane lifetime, defined as the time needed to cross the free energy barrier, is calculated in terms of various parameters. In the third section we focus on transmembrane potential and the cytoskeleton and discuss their effects, along with the memory effect on the phase diagram of membrane stability. In the fourth section we draw a general conclusion.

THE NON-MARKOVIAN STOCHASTIC MODEL OF PORE GROWTH

Here we develop a model for the stochastic dynamics of a pore. The dynamics is affected not only by the membrane matrix in which the pore is embedded, but also by other environmental factors, e.g., ambient solvent and cytoskeletal network (Fig. 1). In considering the membrane effect on the dynamics, we will here focus on the fluid part of the membrane (i.e., fluid membrane), leaving the effect of cytoskeletal meshwork to be discussed in a later section.

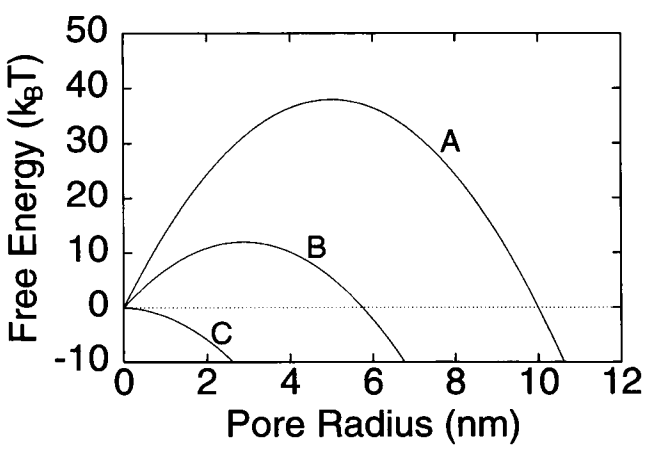

FIGURE 2 The free energy $\mathcal{A}(r) = 2\pi\lambda r - \pi\sigma r^2$ of pore formation with radius r for different transmembrane potential differences (A: $U = 0$ mV; B: $U = 200$ mV; C: $U = 300$ mV), with λ and σ given by Eqs. 23 and 24, respectively. $T = 300$K, $\lambda_0 = 1 \times 10^{-11}$ N, and $\sigma_0 = 2 \times 10^{-3}$ N/m.

As a membrane is composed of macromolecules (i.e., lipids), its stress response to an external deformation is not instantaneous but delayed. Its stress delay or relaxation is characterized by a characteristic time τ_η, which assumes the value exceeding molecular scales (Nash et al., 1986; Hochmuth, 1987). Depending on the time scale of deformation, a fluid membrane manifests a dual character, namely, viscoelasticity; for times much shorter than τ_η, the fluid membrane responds as an elastic solid, whereas for times much larger than τ_η, it behaves like a fluid with a high viscosity (Doi and Edwards, 1986).

Consider a pore of cylindrical geometry with radius r (much larger than lipid) and thickness d in a membrane. The radial, damping force on the pore exerted by the fluid membrane and solvent is given as

$$F_D(t) = -\gamma\dot{r}(t) - \int_0^t \zeta(t - t')\dot{r}(t')dt' \tag{3}$$

The first term is the (Markovian) frictional force arising from an instantaneous response of the solvent and membrane on the time scale of pore growth. The second term is the (non-Markovian) force due to the delayed response from membrane matrix, which we regard as a two-dimensional viscoelastic liquid continuum. As given in the Appendix, we obtain it by calculating the hydrodynamic force on the pore (radial stress multiplied by the edge area). Assuming that it decays exponentially with the relaxation time τ_η, the memory function $\zeta(t)$ is given by

$$\zeta(t) = K \exp(-t/\tau_\eta) \tag{4}$$

Here $K \equiv 4\pi\eta d\tau_\eta^{-1}$ is a measure of the memory strength, and η is the shear viscosity of the membrane.

For the long times much larger than τ_η or for slow pore growth, the force is frictional:

$$F_D(t) = -(\gamma + \gamma_M)\dot{r}(t), \tag{5}$$

where $\gamma_M \equiv 4\pi\eta d = K\tau_\eta$ is the long-time membrane friction coefficient. Intuitively, γ_M is much larger than γ, the instantaneous friction. For the times much shorter than τ_η or for fast pore growth, the force is given by

$$F_D(t) = -\gamma\dot{r}(t) - K\delta r(t) \tag{6}$$

where $\delta r(t) \equiv r(t) - r(0)$. It is clear in Eq. 6 that the membrane damping force includes a restoring force due to its memory, i.e., the effective membrane elasticity represented by the spring constant K dynamically induced at short times or at short time scales.

In addition, we consider the stochastic force $f(t)$ acting on the pore, which is not accounted for by Eqs. 2 and 3; we

model it as a Gaussian noise, which is related to the memory function via the fluctuation dissipation theorem (FDT):

$$\langle f(t)f(t')\rangle = k_B T[2\gamma\delta(t-t') + \zeta(t-t')] \quad (7)$$

Here $\langle\cdots\rangle$ means the average over an equilibrium ensemble. Equation 7 implies that the $f(t)$ is decomposed into an instantaneous, white noise, and a relatively slow, colored noise. FDT signifies a detailed balance that brings the system to equilibrium in very long times in the absence of external forces. Summing F_A, F_D, and f together, we postulate that the pore radius r is described by the generalized Langevin equation (considering the time scales of growth on which the inertia term can be neglected),

$$-\frac{\partial \mathcal{A}(r)}{\partial r} - \gamma\dot{r}(t) - \int_0^t \zeta(t-t')\dot{r}(t')dt' + f(t) = 0 \quad (8)$$

or more explicitly,

$$k(r-r_B) - \gamma\dot{r}(t) - K\int_0^t \exp\left(-\frac{t-t'}{\tau_\eta}\right)\dot{r}(t')dt' + f(t) = 0 \quad (9)$$

The great distinction of two time scales (as is apparent in Eq. 7) and two magnitudes (γ and γ_M) of the damping is an important condition of our model. It should be noted here although transmembrane potential and cytoskeletal network affect the driving force $F_A = k(r - r_B)$ by modifying $k \equiv 2\pi\sigma$ and $r_B \equiv \lambda/\sigma$, as will be discussed in the next section, they do not modify the other terms above.

This stochastic model enables us to associate the pore growth as a generalized Brownian motion crossing the activation free energy barrier given by $\mathcal{A}(r)$. The escape time $\mathcal{T}$ defined by the mean first passage time from a metastable region $0 < r < r_B$ of the free energy to the region $r > r_B$ is the central object of our study. As the pore with $r > r_B$ undergoes a large irreversible growth, leading to an eventual membrane breakdown, we call this time the membrane lifetime. As shown below, we find that a modern non-Markovian extension of Kramers' theory by Grote and Hynes (1980) and Hänggi and Mojtabai (1982) (GHHM) can be adapted to our model.

GHHM considered a Brownian particle with mass m described by a generalized Langevin equation, which can be written in our terminology:

$$m\ddot{r} = -\int_0^t \zeta(t-t')\dot{r}(t')dt' + k(r-r_B) + f(t) \quad (10)$$

The $f(t)$ is a Gaussian colored noise related to $\zeta(t)$ via FDT:

$$\langle f(t)f(0)\rangle = k_B T\zeta(t) \quad (11)$$

where $\zeta(t)$ is the memory function given by Eq. 4. Provided that $\mathcal{T} \gg \tau_\eta$ as is indeed true in this study, the escape rate $\mathcal{R} \equiv \mathcal{T}^{-1}$ is given by the renormalized version of transition state theory (TST) (see, for a review, Hänggi et al., 1990),

$$\mathcal{R} = \frac{\omega_B^*}{\omega_B}\mathcal{R}_{TST} \quad (12)$$

where $\mathcal{R}_{TST}$ is the escape rate in accordance with classical TST:

$$\mathcal{R}_{TST} = (2\pi\beta m)^{-1/2}\frac{\exp(-\beta\mathcal{A}(r_B))}{\mathcal{Q}}. \quad (13)$$

Here $\beta = 1/k_B T$, $\mathcal{Q} \equiv \int_0^{r_B}\exp(-\beta\mathcal{A}(r))dr$, $\omega_B \equiv -m^{-1}\, d^2\mathcal{A}(r)/dr^2|_{(r=r_B)} = (k/m)^{1/2}$ is the angular frequency at the barrier top $r = r_B$, and ω_B^* is its renormalized value due to the friction effect that the pore experiences on the time scale of its growth. The ratio of these quantities is given by the GHHM generalization of the Kramers' Markovian result:

$$\frac{\omega_B^*}{\omega_B} = \left[\left(\frac{\tilde{\zeta}(\omega_B^*)}{2m\omega_B}\right)^2 + 1\right]^{1/2} - \left(\frac{\tilde{\zeta}(\omega_B^*)}{2m\omega_B}\right) \quad (14)$$

where $\tilde{\zeta}(s)$ is the Laplace transform of $\zeta(t)$ with Laplace variables. m is the mass of the effective Brownian particle corresponding to the fictitious inertia of the pore in radial expansion in our case. However, this bothersome mass disappears in the final expression of escape rate, as it should, because we are concerned with a long time (Smoluchowski dynamics) scale of Brownian motion in which the inertia is irrelevant. On that time scale, $\tilde{\zeta}(\omega_B^*) \gg m\omega_B$, Eqs. 10 and 14 are respectively reduced to

$$-\int_0^t \zeta(t-t')\dot{r}(t')dt' + k(r-r_B) + f(t) = 0 \quad (15)$$

and

$$\frac{\omega_B^*}{\omega_B} = \frac{m\omega_B}{\tilde{\zeta}(\omega_B^*)} \quad (16)$$

With the memory function Eq. 4 inserted, Eq. 16 yields

$$\omega_B^* = \tau_\eta^{-1}(K/k - 1)^{-1} \quad (17)$$

The inequality condition $k > K$, although allowed in the system, leads to negative values for $\mathcal{R}$, as shown in Eq. 17. This inconsistency results from the model Eq. 10 in the Smoluchowski limit ($m\ddot{r} \to 0$), as already pointed out in a different context (Einchcomb and McKane, 1995). This difficulty does not exist when Eq. 15 is replaced by our model Eq. 8 or 9; whereas at $t = 0, f = -k(r - r_B)$ in Eq. 15, $f(t) = -k(r - r_B) + \gamma\dot{r}$ in Eq. 9, so that the stochastic force can retain a rapidly varying component ($\gamma\dot{r}$) in the latter, as it should. With the memory function $\zeta(t)$ replaced by $\zeta(t) + 2\gamma\delta(t)$, and its Laplace transform replaced by $\tilde{\zeta}(\omega_B^*) + \gamma$, we have, instead of Eq. 16,

$$\frac{\omega_B^*}{\omega_B} = \frac{m\omega_B}{\tilde{\zeta}(\omega_B^*) + \gamma} \quad (18)$$

and the escape rate, Eq. 12, which is indeed well defined for $k > K$ and is independent of m.

If we neglect the memory effect, i.e., $K = 0$, the rate is reduced to that of a Markov process given by the well-known Kramer's theory (see, for a review, Hänggi et al., 1990),

$$\mathcal{R} \rightarrow \mathcal{R}_0 = \frac{m\omega_B}{\gamma}\mathcal{R}_{TST} \tag{19}$$

for large friction regime ($\gamma \gg m\omega_B$). This escape rate is apparently proportional to γ^{-1} and $\exp(-\beta\mathcal{A}(r_B))$, known as the Arrhenius factor, but has a preexponential factor depending on the detail of free energy shape.

With the memory function Eq. 4 incorporated, the two roots of ω_B^* in Eq. 18 correspond to the growth and decay modes, also obtainable directly from our generalized Langevin equation (Eq. 8). Only the growth mode has a positive value:

$$\omega_B^* = \frac{k}{2\gamma}\left[\left(1 - \frac{K + \gamma\tau_\eta^{-1}}{k}\right) + \left\{\left(1 - \frac{K + \gamma\tau_\eta^{-1}}{k}\right)^2 + \frac{4\gamma}{k\tau_\eta}\right\}^{1/2}\right] \tag{20}$$

$$\approx \begin{cases} k/\gamma, & k \gg K \\ k/(\gamma\gamma_M)^{1/2}, & k \simeq K \\ k/\gamma_M, & k \lesssim K \end{cases} \tag{21}$$

Because the value of γ/γ_M is very small in our problem, the renormalization ω_B^*/ω_B and hence the escape rate $\mathcal{R}$ in Eq. 12 undergo a sharp crossover near $k = K$, as shown in Eq. 21 and Fig. 3. For $k \gg K$, the $\mathcal{R}$ is reduced to that of Kramer's theory with Markovian friction γ, and membrane viscoelasticity gives no effect on $\mathcal{R}$. For $k \lesssim K$, the membrane medium resists pore growth elastically, reducing the Kramers rate by the ratio γ/γ_M.

The transitional behavior can also be explained in a simple qualitative term by considering the pore dynamics of crossing the free energy barrier $\mathcal{A}(r)$. At a very short time, after which pore state crosses the barrier top, in view of Eq. 6, Eq. 9 is reduced to

$$(k - K)\delta r(t) - \gamma\dot{r}(t) + f(t) \simeq 0 \tag{22}$$

where $\delta r(t) = r(t) - r_B$. When $k > K$, the solution of the above equation shows that the pore will thus grow indefinitely. When $k < K$, on the other hand, the restoring membrane force $-K\delta r(t)$ dominates the instability driving force $k\delta r(t)$, resealing the pore. Therefore, the pore growth is a dynamic transition determined by competition between the "internal (memory-induced) spring" K and the "external (surface tension-induced) spring" k. As k is given by the surface tension, which can be modulated by solvent, transmembrane potential and cytoskeletal meshwork, rich dynamic transitions in membrane stability are expected to occur, depending on the interplay of these effects.

Equation 20, upon substitution into Eq. 12, yields an analytical expression for the escape rate, and hence for the escape time, or the membrane lifetime defined by $\mathcal{T} \equiv \mathcal{R}^{-1}$. $\mathcal{T}$ expresses the stability of the membrane in terms of various measurable membrane parameters. In addition to the static parameters such as surface tension σ and line tension λ, it involves the dynamic parameters such as membrane stress relaxation time τ_η and viscosity η. We found also it crucial to incorporate the instantaneous friction coefficient γ, the small value of which compared with γ_M, although challenging to determine experimentally, gives rise to a sharp transition to membrane stability induced by the membrane memory or viscoelasticity. This dynamically induced stability gives a significant modification of the previous stability criteria (Abidor et al., 1979; Winterhalter and Helfrich, 1987), given only by the free energy, i.e., the Arrhenius factor. In the following we discuss these modifications and new features, for the membrane in the presence of a transmembrane electric potential and a cytoskeletal network inside the cell.

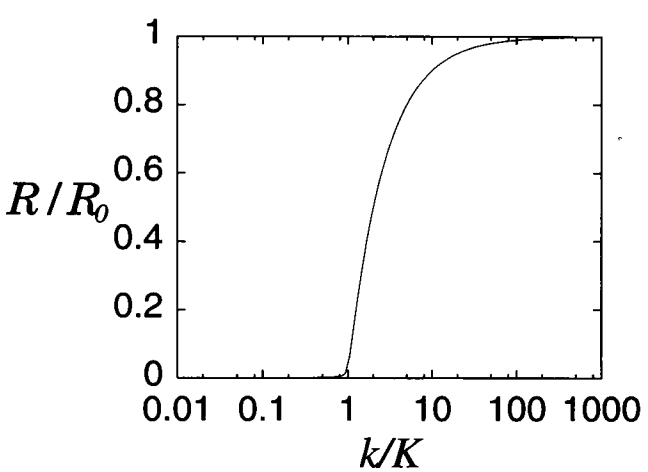

FIGURE 3 Ratio of the escape rate $\mathcal{R}$ with finite memory strength K to that with $K = 0(\gamma/\gamma_M = 10^{-5})$. The escape (growth) rate is sharply reduced by membrane memory for $K > k$.

EFFECTS OF TRANSMEMBRANE POTENTIAL AND CYTOSKELETAL NETWORK

In living cells, a natural resting membrane potential difference of the magnitude $U \lesssim 100$ mV is maintained across membranes because of ionic imbalance. For electroporation, the externally applied potentials can be much higher and are usually in the form of pulse and step. Here we investigate the effect of constant transmembrane potential U. Winterhalter and Helfrich (WH) (1987) treated the water-filled pore as a conducting disk embedded in a dielectric continuum (membrane) of thickness d, and obtained the edge energy and surface tension modified from the unperturbed values λ_0, σ_0:

$$\lambda(U) = \lambda_0 - \frac{\epsilon_W U^2}{2\pi} \tag{23}$$

$$\sigma(U) = \sigma_0 - \frac{\epsilon_L U^2}{2d} \tag{24}$$

Here $\epsilon_L \simeq 2\epsilon_0$, $\epsilon_W \simeq 80\epsilon_0$, ϵ_0 are the dielectric constants of the lipid membrane, water, and vacuum, respectively. It should be mentioned (Wilhelm et al., 1993; Winterhalter et al., 1995) that the dependence on U is different from what is usually considered in conventional analysis for electroporation (Neumann et al., 1989),

$$\lambda(U) = \lambda_0 \tag{25}$$

$$\sigma(U) = \sigma_0 + \frac{(\epsilon_W - \epsilon_L)}{2d} U^2 \tag{26}$$

Rather than a simple dielectric condenser energy yielding Eq. 26, WH more realistically considered the field distortion due to a water-filled pore as a conductor and calculated the Maxwell stress, yielding Eqs. 23 and 24. Whereas the conventional model attributes field-induced membrane instability to an increase in surface tension as the field increases (Eq. 26), the WH model attributes it mostly to a decrease in the line tension (Eq. 23). We adopt this WH model for our problem.

As U increases, both λ and σ decrease. Beyond the threshold values defined by $U_0 = (2\pi\lambda_0/\epsilon_W)^{1/2}$ and $U_\infty = (2d\sigma_0/\epsilon_L)^{1/2}$, λ and σ change their signs to negative. Considering just the associated free energy changes (shown in the boxes in Fig. 4), we can give a stability criterion that can be seen in the phase diagram. With U_0 fixed, the phase diagram is explained as follows. If $k_0 \equiv 2\pi\sigma_0$ is larger than k_c, the critical value defined by the value of k_0 at which $U_0 = U_\infty$, the metastable (MS) membrane tends to be more unstable (US) as U increases to U_0 of vanishing lifetime; if the field increases further beyond U_0, it tends to remain unstable until the potential U_∞, above which it attains stability with a finite pore radius (Fig. 4). If k_0 is smaller than k_c, the membrane tends to be more stable (S) against the pore growth as U increases to U_∞, where its lifetime is infinity. Thus $k_c \equiv 2\pi\sigma_c$ with $\sigma_c \equiv \pi\epsilon_L\lambda_0/\epsilon_W d$ defines the critical surface tension, above (below) which an increase in the field destabilizes (stabilizes) the membrane. This bifurcative behavior is a consequence of the WH model.

With the memory effect, the transitional behavior shown in Eq. 20 and in Fig. 3, superimposed on the above picture, we find the phase diagram is changed to Fig. 5. The new phase boundary $U_K(k_0)$, obtained from Eq. 24 and the crossover condition $k(U_K) \equiv 2\pi\sigma(U_K) = K$ discussed earlier, now introduces the quasistable (QS) region induced by memory effect, thereby enhancing the overall domain of stability (Fig. 5). In this QS region, previously identified as a metastable or unstable region, the membrane stability is enhanced in accordance with Eq. 21. Here we define the shifted value k_c' by the value k_0 at which $U_0 = U_K$, and the corresponding shifted critical state c'.

In Fig. 6, the dependence of $\mathcal{T}$ upon U in a metastable (MS) phase as calculated from Eq. 12 is plotted for various values of k_0 larger than k_c, K, and k_c'. The membrane parameters chosen here are typical values taken from Freeman et al. (1994) and Winterhalter et al. (1995), in which it is shown that $k_c < K < k_c' < k_0$, with each value having the same order of magnitude. Fig. 6 shows the simple destabilizing effect of membrane potential until it increases to $U_0 \simeq 300$ mV, corresponding to zero lifetime. In this domain of parameters, the Markovian theory of Kramers is valid, and such dependence on U is expected from the Arrhenius factor. This destabilizing effect of transmembrane potential is consistent with other theories (Sugar, 1989) and with experiments (Chernomordik et al., 1987), although the latter have usually been done with the potential in the form of a step.

As the σ_0, the surface tension in the absence of potential, is proportional to the difference in the lipid chemical potential between the membrane and the solvent (Kashchiev, 1987), and thus is affected by the cytoskeletal network discussed next, it can assume a range of smaller values than that considered above, depending on the environment. To demonstrate how sensitively the membrane stability depends on these environmental factors coupled with the memory (non-Markovian) effect, we consider a range of small values of k_0 near k_c, K, and k_c', as well as values of γ, λ_0 and η given in Fig. 7. It shows diverse behaviors of

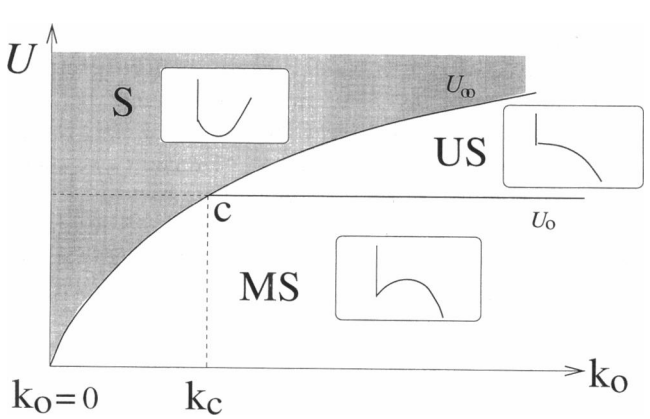

FIGURE 4 Phase diagram in terms of $k_0 = 2\pi\sigma_0$ and transmembrane potential difference U (S, stable; MS, metastable; US, unstable). Figures in small boxes show free energy curves for the corresponding three phases.

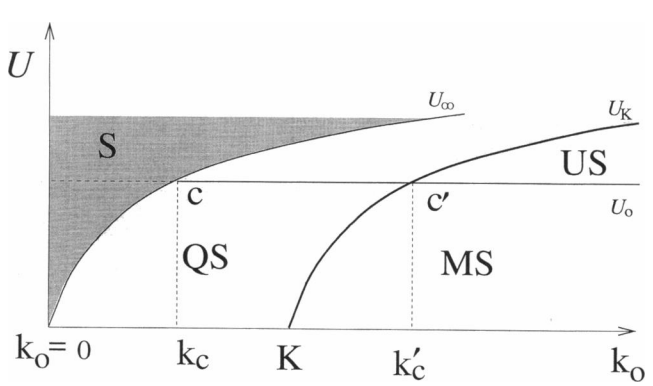

FIGURE 5 Phase diagram in terms of $k_0 = 2\pi\sigma_0$ and transmembrane potential difference U (S, stable; MS, metastable; US, unstable; QS, quasistable). The membrane memory effect (Eq. 4) introduces a new phase boundary ($U = U_K(k_0)$).

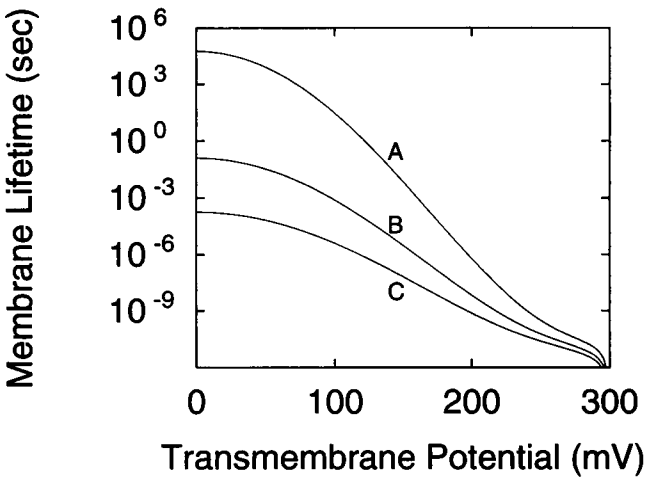

FIGURE 6 Membrane lifetime versus transmembrane potential difference. The values for σ_0 and λ_0 are given below (Freeman et al., 1994), and η is taken from Hochmuth (1987). The electric field simply destabilizes the cell membrane. $\gamma = 5.0 \times 10^{-13}$ N s/m, $\eta = 1.0$ kg/m s, $d = 4 \times 10^{-9}$ m, $\tau_\eta = 10^{-6}$ s, $T = 300$K, $\lambda_0 = 10^{-11}$ N. (*A*) $\sigma_0 = 2.0 \times 10^{-3}$ N/m. (*B*) $\sigma_0 = 3.0 \times 10^{-3}$ N/m. (*C*) $\sigma_0 = 4.0 \times 10^{-3}$ N/m.

membrane lifetimes as U increases. The curves A, B, and C correspond to the phases with the values of k_0 in the ranges $k_0 < k_c$, $k_c < k_0 < K$, $K < k_0 < k_c'$, respectively, belonging to non-Markovian domains, and curve D corresponds to the phase with k_0 larger than k_c', belonging to a Markovian domain. Interesting bifurcative behaviors (stability for A and instability for B) follow for the values of k_0 near k_c (the critical point c in Fig. 5), corresponding to the transmembrane potential given by $U_0 \simeq 100$ mV. This consideration suffices to show that the membrane can undergo a variety of sharp dynamic transitions due to modulation of surface

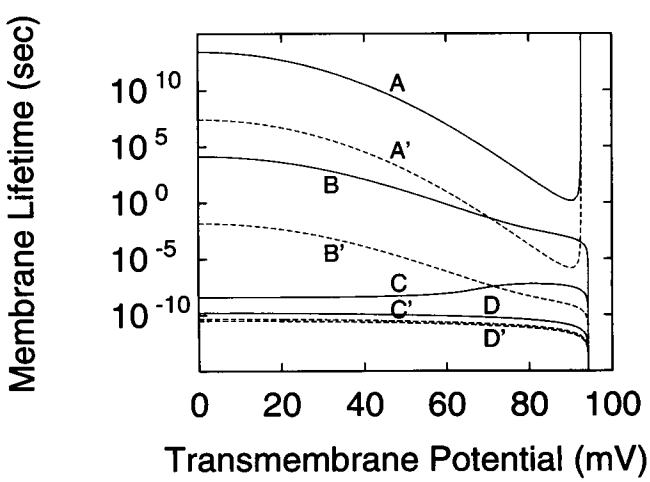

FIGURE 7 Membrane lifetime versus transmembrane potential difference for small values of σ_0, with $\lambda_0 = 10^{-12}$ N, and holding other parameters the same as in Fig. 6. (*A*) $\sigma_0 = 1.9 \times 10^{-5}$ N/m. (*B*) $\sigma_0 = 4.0 \times 10^{-5}$ N/m. (*C*) $\sigma_0 = 8.1 \times 10^{-4}$ N/m. (*D*) $\sigma_0 = 1.0 \times 10^{-3}$ N/m. A bifurcative behavior is observed around $U_0 \simeq 100$ mV. The dashed lines are the corresponding Markovian results, where the memory term is neglected. Enhanced stability due to memory can be seen in curves A and B.

tension induced by the small fluctuations in solvent environment near critical situations ($k_0 = k_c$). Also shown is significant enhancement of stability for the QS cases A, B over the Markovian predictions indicated by the dashed lines A', B'.

An important environmental factor that affects the pore growth is the polymer meshwork called cytoskeleton anchored with the intracellular side of membrane. A qualitative argument on stability induced by the cytoskeleton was given by Chang and Reese (1990). To analyze the effect quantitatively we consider that, assuming the permanent cytoskeletal anchorage, the additional free energy cost for pore formation due to the meshwork is given as $\mathcal{A}_{cyto}(r) = \frac{1}{2}K_{cyto}r^2$. Here the spring constant K_{cyto} is related to the cytoskeletal contribution to shear modulus G_{cyto} by $K_{cyto} = 4\pi G_{cyto}d$. (Just as the steady-state frictional force on the pore immersed in a viscous media of shear viscosity η is given by (Appendix) $F = -4\pi\eta d\tau_\eta^{-1}\dot{r}$, the restoring force associated with enlarging pore radius by δr in an elastic media of shear modulus G is given by $F = -4\pi G d\delta\dot{r}$. This is due to the similarity between the elastic and viscous hydrodynamic constitutive relations.) This effect of the cytoskeletal network, as seen in Eq. 1, is to stabilize the membrane by reducing the surface tension, which we can analytically incorporate by replacing k_0 by $k_0 - K_{cyto}$ in the escape rate (Eq. 12). Qualitatively, the phase boundary $U_K(k_0)$ in the phase diagram (Fig. 5) shifts to the right, and as a result, the cytoskeleton further enlarges the stable region. If the shifted value, $k_0 - K_{cyto}$, which can be called as the effective surface tension, can be a small value as considered in the preceding paragraph, Fig. 7 A and B suggests that sharp transitions to stability (from B to A) can be induced by cytoskeletal modulation at a resting membrane potential of $U \simeq 100$ mV. Also implied by B, C, and D of the figure is the opposite possibility that the surface tension increases beyond that of A by cytoskeletal modulation and solvent fluctuation, even minute, can initiate sudden pore growth spontaneously to bring about the translocation of macromolecules directly through the lipid bilayer at that potential. The cytoskeleton-induced reduction of surface tension can, therefore, cause the membrane to be susceptible to the memory effect discussed earlier.

We know of no experimental data to verify these theoretical suggestions, as all of these results are specific to constant potentials, which can be as low as the resting potential. It would be interesting to correlate experiments with the theoretical predictions given here by using a voltage clamp wherein the potential is kept fixed during the whole pore growth process, and by controlling the relevant membrane parameters, especially the low surface tensions modulated by the cytoskeletal meshwork.

SUMMARY AND CONCLUDING REMARKS

Using statistical physics of non-Markovian stochastic process crossing over free energy barrier, we have determined

analytically the lifetime of a pore-induced metastable membrane and assessed the phase diagram for its stability, in terms of membrane and environmental effects as well as the transmembrane potential. The membrane stability can sensitively depend upon these factors and, as we have found, has an interesting dynamic phase transition as the result of competitions between these factors. Whereas the memory effect is manifested as dynamically induced elasticity over short times, and the cytoskeletal effect tends to stabilize the membrane against pore growth, constant electric fields stabilize or destabilize the membrane, depending upon the strength. Owing to diversity of biological systems and of membrane parameters, the pore states near the critical points c and c' (in Fig. 5) can be accessible. And, there, because of the enormous sensitivity to fluctuations, the parameter fluctuations characteristic of the soft matter in mesoscopic level will affect the fates of pores in a biomembrane in various ways.

APPENDIX: HYDRODYNAMIC CALCULATION OF THE MEMORY FRICTION AGAINST PORE GROWTH

In this appendix we calculate the time-dependent response (damping) of membrane matrix against pore growth in terms of membrane parameters, i.e., the memory function (Eq. 4). To incorporate the viscoelasticity of membrane, we start from two-dimensional generalized hydrodynamics in the geometry shown in Fig. 8. Considering small deviations of hydrodynamic field quantities such as density, fluid velocity, pressure from their equilibrium values (e.g., for the mass density of the fluid, $\rho = \rho_{eq} + \delta\rho$), the linearized hydrodynamic equations read

$$-\frac{\partial}{\partial t}\delta\rho(\mathbf{r}, t) = \rho_{eq}\nabla\cdot\mathbf{u}(\mathbf{r}, t) \tag{A1}$$

$$-\rho_{eq}\frac{\partial}{\partial t}\mathbf{u}(\mathbf{r}, t) = \nabla\cdot\mathbf{\Pi}(\mathbf{r}, t) \tag{A2}$$

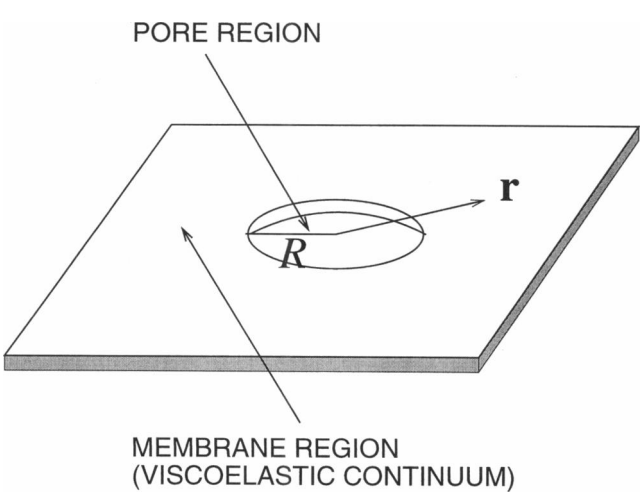

FIGURE 8 The geometry of a pore in a quasi-two-dimensional membrane.

Because of the viscoelasticity of membrane Π, the stress tensor has the generalized form

$$\mathbf{\Pi}_{ij}(\mathbf{r}, t) = \delta P(\mathbf{r}, t)\delta_{ij} - \int_0^\infty dt'[\eta^B(t-t')\nabla\cdot\mathbf{u}(\mathbf{r}, t')\delta_{ij}]$$

$$-\int_0^\infty dt'\left[\eta(t-t')\left(\nabla_i u_j(\mathbf{r}, t') + \nabla_j u_i(\mathbf{r}, t') - \frac{2}{3}\nabla\cdot\mathbf{u}(\mathbf{r}, t')\delta_{ij}\right)\right] \tag{A3}$$

where $\eta(t)$ and $\eta^B(t)$ are the time dependent shear relaxation modulus and bulk relaxation modulus, respectively.

Taking the Laplace transforms of these equations with Laplace variable s yields

$$-s\delta\rho(\mathbf{r}, s) = \rho_{eq}\nabla\cdot\mathbf{u}(\mathbf{r}, s) \tag{A4}$$

$$\rho_{eq}s\mathbf{u}(\mathbf{r}, s) = \left[\frac{\rho_{eq}c^2}{s} + \frac{4}{3}\eta(s) + \eta^B(s)\right]\nabla\nabla\cdot\mathbf{u}(\mathbf{r}, s) - \eta(s)\nabla\times\nabla\times\mathbf{u}(\mathbf{r}, s) \tag{A5}$$

in which the following thermodynamic relation was used:

$$\nabla\delta P(\mathbf{r}, t) \approx \frac{\partial P}{\partial\rho}\nabla\delta\rho(\mathbf{r}, t) = c^2\nabla\delta\rho(\mathbf{r}, t) \tag{A6}$$

where c is the sound velocity of the medium. From the symmetry consideration, $\mathbf{u}(\mathbf{r}, t)$ has only a radial component that is a function only of r:

$$\mathbf{u}(\mathbf{r}, t) = u_r(r, t)\hat{r} \tag{A7}$$

Substituting this equation into Eq. A5 yields an ordinary differential equation for $u_r(r, s)$, whose solution is a modified Bessel function of order 1, as

$$u_r(r, s) = A(s)K_1(\kappa(s)r) \tag{A8}$$

where the first kind of modified Bessel function $I_1(\kappa(s)r)$ is excluded to make the velocity finite at $r = \infty$, and $\kappa(s)$ is defined as follows:

$$\kappa(s) = \sqrt{\frac{\rho_{eq}s}{(c^2/s)\rho_{eq} + (4/3)\eta(s) + \eta^B(s)}} \tag{A9}$$

We denote the pore expansion rate as

$$V(t) = \frac{dR(t)}{dt} \tag{A10}$$

Then the boundary condition at $r = R(t)$ reads

$$u_r(r = R(t), t) = V(t) \tag{A11}$$

Considering the linear response of radial velocity to the expansion rate of a pore, we can write

$$u_r(r, s) = B(s)K_1(\kappa(s)r) \times V(s) \tag{A12}$$

where $V(s)$ is the Laplace transform of pore expansion rate. From Eq. A11, the unknown function $B(s)$ could be determined as

$$B(s) \simeq \frac{1}{K_1(\kappa(s)R)} \tag{A13}$$

Because the radius of a pore is a slowly varying degree of freedom, it remains nearly stationary within the microscopic relaxation time. Hence the above approximation will do fine. From the knowledge of $u_r(r, t)$, we can calculate from Eq. A3 the stress distribution $\Pi(r, t)$, which is expected to have only a nonvanishing component Π_{rr} from the symmetry consideration. After a little algebra, Π_{rr} can be obtained as follows:

$$\Pi_{rr}(r, s) = \frac{\kappa(s)V(s)}{K_1(\kappa(s)r)} \cdot \left[\left(\frac{c^2}{s}\rho_{eq} + \frac{1}{3}\eta(s) + \eta^B(s)\right)K_0(\kappa(s)r) + \eta(s)K_2(\kappa(s)r)\right] \quad \text{(A14)}$$

Integrating the radial stress over the area of pore boundary, one obtains the radial force,

$$F(t) = -\int_{\text{pore boundary}} \hat{r} \cdot \Pi(r, t) \cdot \hat{r} dA = -2\pi R d \mathcal{L}^{-1}[\Pi_{rr}(R, s)] \quad \text{(A15)}$$

where $\mathcal{L}^{-1}[f(s)]$ denotes inverse Laplace transform of $f(s)$. In terms of memory function $\zeta(t)$, frictional force can be represented as a convolution integral coupled to the pore expansion rate:

$$F(t) = -\int_0^t \zeta(t - t')\frac{dR(t')}{dt'}dt' \quad \text{(A16)}$$

which can be written upon a Laplace transform as

$$F(s) = -\zeta(s)V(s) \quad \text{(A17)}$$

Combining these expressions, memory function $\zeta(t)$ is given by

$$\zeta(t) = 2\pi R d \mathcal{L}^{-1}\left[\frac{\Pi_{rr}(R, s)}{V(s)}\right] \quad \text{(A18)}$$

Taking $s \to 0$ in its Laplace transform, the integration of the memory function yields

$$\lim_{s\to 0} \zeta(s) \equiv \int_0^\infty \zeta(t)dt \quad \text{(A19)}$$

$$= 4\pi d\eta(s \to 0) \quad \text{(A20)}$$

$$= 4\pi\eta d \quad \text{(A21)}$$

where the zero frequency shear viscosity is expressed as η. From this expression, we can see that the bulk relaxation modulus $\eta^B(t)$ plays no role on the frictional force over long times. Incorporating all of the relaxation modes into a single mode that is assumed to be exponentially decaying, we can deduce the memory function as

$$\zeta(t) = \frac{4\pi\eta d}{\tau_\eta}\exp(-t/\tau_\eta) \quad \text{(A22)}$$

We acknowledge the support from the BSRI program funded by the Ministry of Education of Korea, and POSTECH BSRI/Special Fund.

REFERENCES

Abidor, I. G., V. B. Arakelyan, L. V. Chernomordik, Y. A. Chizmadzhev, V. F. Pastushenko, and M. R. Tarasevich. 1979. Electric breakdown of bilayer lipid membrane. I. The main experimental facts and their qualitative discussions. *Bioelectrochem. Bioenerg.* 6:37–52.

Chang, D. C., B. M. Chassy, J. A. Saunders, and A. E. Sowers, editors. 1992. Guide to Electroporation and Electrofusion. Academic Press, New York.

Chang, D. C., and T. S. Reese. 1990. Changes in membrane structure induced by electroporation as revealed by rapid-freezing electron microscopy. *Biophys. J.* 58:1–12.

Chernomordik, L. V., G. B. Melikyan, and Y. A. Chizmadzhev. 1987. Biomembrane fusion: a new concept derived from model studies using two interacting planar lipid bilayers. *Biochim. Biophys. Acta.* 906: 309–352.

Dimitrov, D. S. 1984. Electric field-induced breakdown of lipid bilayers and cell membranes: a thin viscoelastic film model. *J. Membr. Biol.* 78:53–60.

Doi, M., and S. F. Edwards. 1986. The Theory of Polymer Dynamics. Oxford University Press, New York.

Einchcomb, S. J. B., and A. J. McKane. 1995. Optimum paths for systems subject to internal noise. *Physica.* A216:128–139.

Freeman, S. A., M. A. Wang, and J. C. Weaver. 1994. Theory of electroporation of planar bilayer membranes: prediction of aqueous area, change in capacitance, and pore-pore separation. *Biophys. J.* 67:42–56.

Grote, R. F., and J. T. Hynes. 1980. The stable state picture of chemical reactions. II. Rate constants for condensed and gas phase reaction models. *J. Chem. Phys.* 73:2715–2732.

Hänggi, P., and F. Mojtabai. 1982. Thermally activated escape rate in presence of long-time memory. *Phys. Rev.* A26:1168–1170.

Hänggi, P., P. Talkner, and M. Borkovec. 1990. Reaction-rate theory: fifty years after Kramers. *Rev. Mod. Phys.* 62:251–341.

Hochmuth, M. 1987. Properties of red blood cells. *In* Handbook of Bioengineering. R. Skalak and S. Chien, editors. McGraw-Hill, New York.

Kashchiev, D. 1987. On the stability of membrane, foam and emulsion bilayers with respect to rupture by hole nucleation. *Colloid Polymer Sci.* 265:436–441.

Litster, J. D. 1975. Stability of lipid bilayers and red blood cell membranes. *Phys. Lett.* A53:193–194.

Nash, G. B., R. Tran-Son-Tay, and H. J. Meiselman. 1986. Influence of preparative procedures on the membrane viscoelasticity of human red cell ghosts. *Biochim. Biophys. Acta.* 855:105–114.

Neumann, E., A. E. Sowers, and C. A. Jordan, editors. 1989. Electroporation and Electrofusion in Cell Biology. Plenum Press, New York.

Sackmann, E., J. Käs, and J. Räder. 1993. On shape transformations and shape fluctuations of cellular compartments and vesicles. *Physica Scripta.* T49:111–118.

Safran, S. A., and J. Klein. 1993. Surface instability of viscoelastic thin film. *J. Phys. II (France).* 3:749–757.

Sugar, I. P. 1989. Stochastic model of electric field-induced membrane pores. *In* Electroporation and Electrofusion in Cell Biology. Plenum Press, New York.

Sugar, I. P., and E. Neumann. 1984. Stochastic model for electric field-induced membrane pores electroporation. *Biophys. Chem.* 19:211–225.

Tsong, T. Y. 1991. Electroporation of cell membranes. *Biophys. J.* 60: 297–306.

Wilhelm, C., M. Winterhalter, U. Zimmermann, and R. Benz. 1993. Kinetics of pore size during irreversible electrical breakdown of lipid bilayer membranes. *Biophys. J.* 64:121–128.

Winterhalter, M., and W. Helfrich. 1987. Effect of voltage on pores in membranes. *Phys. Rev.* A36:5874–5876.

Winterhalter, M., et al. 1995. *In* Electromanipulation of Cells. U. Zimmermann and G. A. Neil, editors.